Neutron Star Crusts and GW physics

M. Ángeles Pérez García
Department of Fundamental Physics & IUFFyM,
University of Salamanca, Spain

June 10, 2021

NS asymmetry as GW emission source

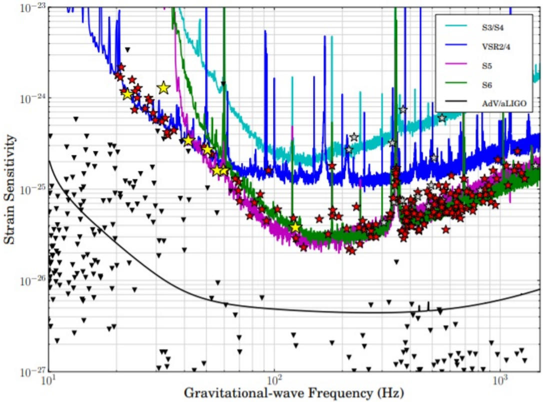

Aasi et al, 2014

fast-spinning NS: $h_0 = 10^{-26}\left(\frac{\epsilon}{10^{-6}}\right)\left(\frac{I_{zz}}{10^{38}\,\mathrm{kg\,m^2}}\right)\left(\frac{\nu}{50\,\mathrm{Hz}}\right)^2\left(\frac{1\,\mathrm{Kpc}}{d}\right)$

ellipticity in asymmetric NSs

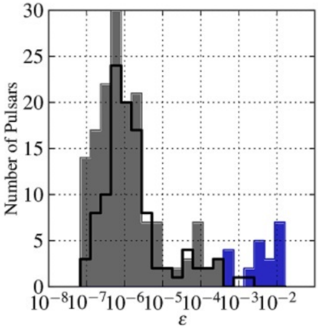

LIGO S5, S6 and Virgo VSR2, VSR4 data

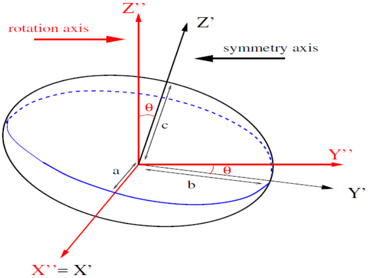

- A rotating NS generates GWs if it has some long-living axial asymmetry $\delta R/R$: mountains, glitches, precession, osc. modes, magnetic deformations.
- ellipticity $\epsilon = \frac{I_{xx} - I_{yy}}{I_{zz}}$

NS structure

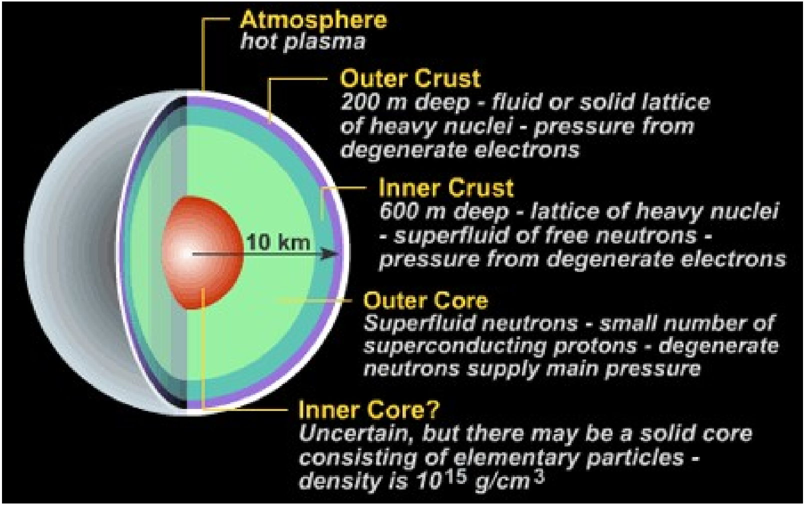

Inhomogeneous crust: PASTA phases

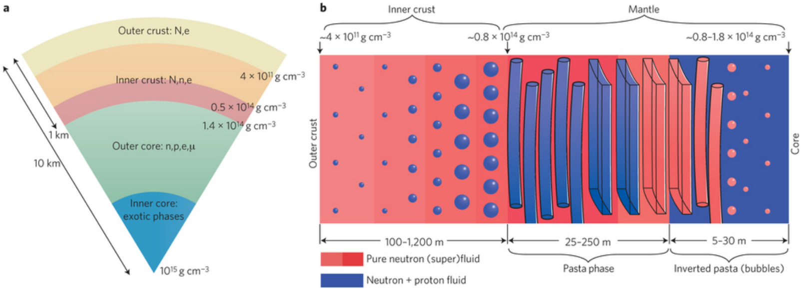

Source: COMPSTAR outreach

- Microscopic models must reflect correlations (also defects or impurities) → extract elastic properties → GW amplitude h_0.
- Microscopic Many-body calculations provide correlations at high order

Simulations in a box with MD

Nuclear dynamics are solved using a thermostat hamiltonian with kinetic and 2B (+3B) potential at finite T and density.

$$H_{\rm NH} = \sum_{i=1}^{A} \frac{\mathbf{P}_i^2}{2m_i} + \sum_{i,j} V_{ij}^{(2)} + \sum_{i,j,k} V_{ijk}^{(3)} + \frac{s^2 p_s^2}{2Q} + g\frac{\ln s}{\beta} \tag{1}$$

where 2B includes hadronic, electromagnetic interaction **screened in the medium**

$$\begin{aligned}
V_{\rm had} &= \sum_{i<j} a e^{-R_{ij}^2/\Lambda} + \left[b + c\tau_i\tau_j\right] e^{-R_{ij}^2/2\Lambda} \\
V_{\rm Debye} &= \sum_{i<j} \frac{e^2}{R_{ij}} e^{-R_{ij}/\lambda_e} \frac{(1+\tau_i)}{2}\frac{(1+\tau_j)}{2} \\
V_{\rm Pauli} &= d\left(\frac{\hbar}{q_0 p_0}\right)^3 \sum_{i,j(\neq i)} \exp\left[-\frac{(R_{ij})^2}{2q_0^2} - \frac{(P_{ij})^2}{2p_0^2}\right] \delta_{\tau_i\tau_j}\delta_{\sigma_i\sigma_j}
\end{aligned} \tag{2}$$

and 3B with a suitable $V_{ijk}^{(3)}$

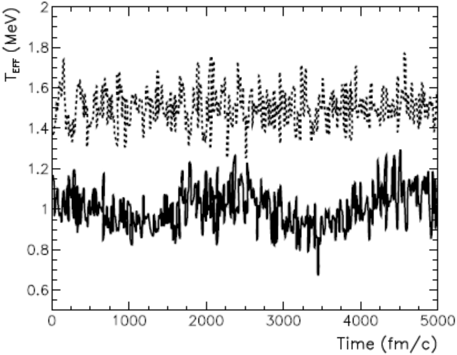

Thermal bath: better T control in the NVT system than rescaling

$n_b = 0.016\,\mathrm{fm}^{-3}$, $Y_e = 0.2$ for $Q = 10^6\mathrm{MeV}(\mathrm{fm/c})^2$ (upper) and $Q = 10^8\mathrm{MeV}(\mathrm{fm/c})^2$ (lower) [Pérez-García et al 2018]

Lower densities in neutron rich pasta

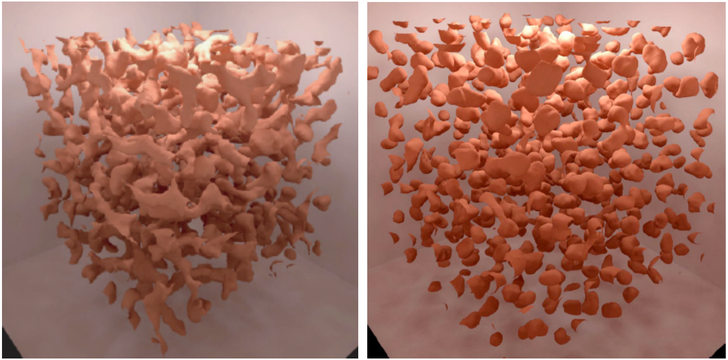

$0.03 fm^{-3}$ proton density isosurface
$n_b = 0.05\ fm^{-3}$ (left) and $n_b = 0.025\ fm^{-3}$ (right).
Watanabe et al 2003, Horowitz, Pérez-García et al. 2004,2005, Caplan et al 2018 and more

Convergence: single ion approximation

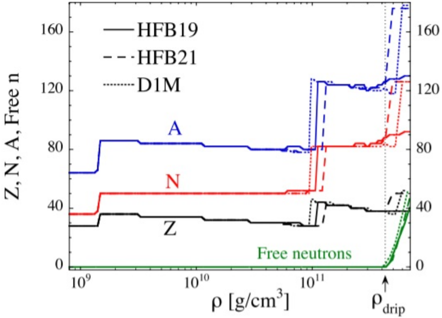

Fig. 1. Ground-state composition (charge, neutron and mass numbers as well as free neutrons) of the outer crust and of the shallow layers of the inner crust as a function of the density. Predictions with HFB-19 masses (solid lines) (Goriely et al. 2010) are compared with those obtained with the D1M masses (dotted lines) (Goriely et al. 2009). Experimental masses (Audi et al. 2003, 2010) are used whenever available.

Goriely et al., 2010.

Ions in a degenerate e^- Fermi sea: Ewald sum

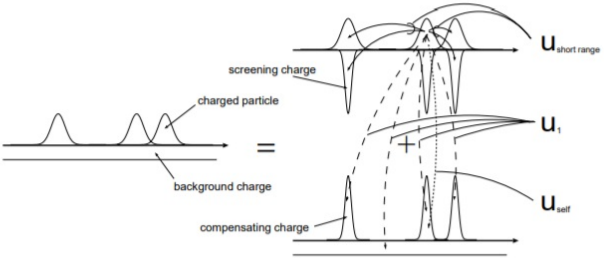

Watanabe et al., 2013.

- Coulomb parameter $\Gamma = (Ze)^2/ak_BT$, $a/L = (3/4\pi N)^{1/3}$. Melting condition: $\Gamma > 175$.
- In-medium: Debye interaction $\frac{1}{R_{ij}} e^{-R_{ij}/\lambda_e}$ with electron screening length $\lambda_e = \frac{1}{2k_{Fe}} \sqrt{\frac{\pi}{\alpha}}$ and Gaussian ionic charges $\rho(r) \sim e^{-r^2/\Lambda}$.

Outer crust: single ion approximation

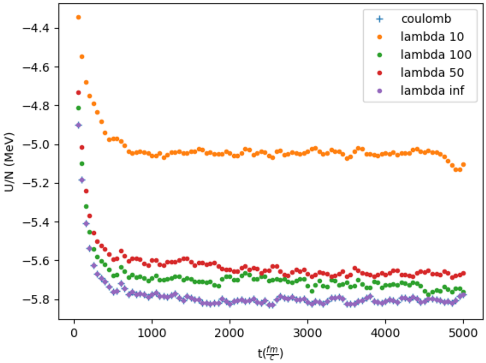

PG, Barba, Albertus in prep 2021.

Summing at all orders in-medium potentials

Contribution from real and reciprocal $\vec{h}$ space (for example in pure Coulomb)

$$U_{\text{real}} = \sum_i Q_i \sum_{j>i} Q_j \frac{\text{erfc}(\kappa r_{ij})}{r_{ij}}$$

$$U_{\text{recip}} = \frac{4\pi}{V} \sum_{h>0}^{\infty} \frac{e^{-h^2/4\kappa^2}}{h^2} \left(\left[\sum_i Q_i \cos\left(\vec{h}\cdot\vec{r_i}\right) \right]^2 + \left[\sum_i Q_i \sin\left(\vec{h}\cdot\vec{r_i}\right) \right]^2 \right)$$

where $\vec{h} = 2\pi \hat{H}^{-1}\vec{n}$, $\vec{n} = (n_x, n_y, n_z)$ and $V = \det(\hat{H})$ is the cell volume.

Corrected energy: $U = U_{\text{real}} + U_{\text{recip}} - U_{\text{self}}$

This will translate into the forces appearing in the **STRESS TENSOR**.

Charged Multipoles $\theta_{\alpha\beta}$

Allowed Nuclear Multipole Moments as a function of Nuclear Spin I

Nuclear Spin	$l=0$ monopole	$l=1$ dipole	$l=2$ quadrupole	$l=3$ octapole	$l=4$ hexadecapole
$I=0$	electric	0	0	0	0
$I=\frac{1}{2}$	electric	magnetic	0	0	0
$I=1$	electric	magnetic	electric	0	0
$I=\frac{3}{2}$	electric	magnetic	electric	magnetic	0
$I=2$	electric	magnetic	electric	magnetic	electric

Electric Quadrupole Moment, Q_I
describes shape of nucleus

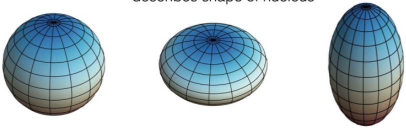

Sphere $Q_I = 0$ | Oblate Spheroid $Q_I < 0$ | Prolate Spheroid $Q_I > 0$

$$U_{Coul} = \sum_i \sum_{j>i} \left(Q_i T_{ij} Q_j + \frac{1}{3} Q_i T_{ij}^{\alpha\beta} \theta_{j\alpha\beta} + \frac{1}{3} Q_j T_{ij}^{\alpha\beta} \theta_{i\alpha\beta} \right).$$

where $T_{ij} = \frac{1}{R_{ij}}$, $T_{ij}^{\alpha\beta} = \nabla_\alpha T_{ij}^{\beta} = \frac{3R_{ij,\alpha}R_{ij,\beta} - R_{ij}^2 \delta_{\alpha\beta}}{R_{ij}^5}$

Stress in the NS crust (pure Coulomb)

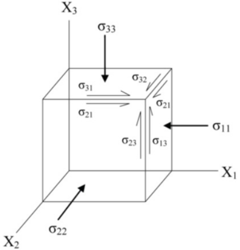

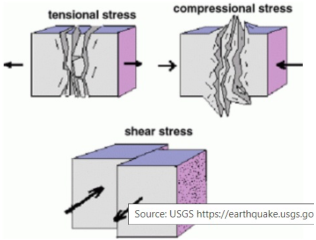

$$\sigma^{\rm tot}_{\alpha\beta} = \frac{1}{V}\sum_i M_i \dot{R}_{i\alpha}\dot{R}_{j\beta} + \sigma_{{\rm real},\alpha\beta} + \sigma_{{\rm recip}\ ,\alpha\beta}$$

$$\sigma^{\rm real}_{\alpha\beta} = \tfrac{1}{2V}\textstyle\sum_{i,j\neq i}\left(F^{\rm real}_{ij,\alpha}R_{ij,\beta} + F^{\rm real}_{ij,\beta}R_{ij,\alpha}\right),$$

$$\sigma^{QQ}_{{\rm recip}\ ,\alpha\beta} = \frac{4\pi}{V^2}\sum_{h>0}^{\infty}\frac{e^{-h^2/4\kappa^2}}{h^2}\left(\delta_{\alpha\beta} - 2\frac{1+\frac{h^2}{4\kappa^2}}{h^2}h_\alpha h_\beta\right)$$

$$\times\left(\left[\sum_i Q_i\cos\left(\vec{h}\cdot\vec{R}_i\right)\right]^2 + \left[\sum_i Q_i\sin\left(\vec{h}\cdot\vec{R}_i\right)\right]^2\right)$$

Non Ewald calculations with Hadrons

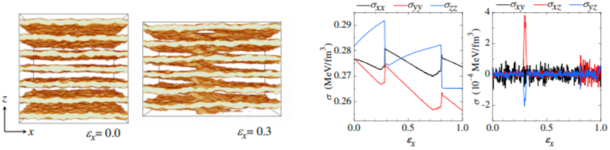

(b) Tensile deformation pulling lasagna sheets laterally while compressing them

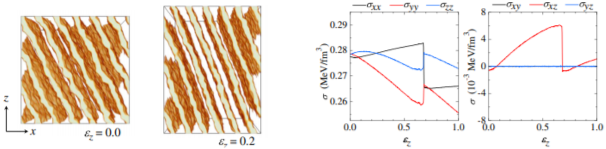

(c) Lasagna sheets experiencing both tensile and shear strains

Pasta max. breaking strains of order 0.1 MeV/fm^3. $n_b = 0.05$ fm^{-3} , $Y_p = 0.4$. Caplan et al., 2018.

$$\Phi_{22,\max} = 2.4 \times 10^{39} g\, \mathrm{cm}^2 \left(\frac{\sigma_{\max}}{10^{-1}}\right) \left(\frac{R}{10\,\mathrm{km}}\right)^{6.26} \left(\frac{1.4 M_\odot}{M}\right)^{1.2}$$

$10^{-5} < \sigma_{\max} < 10^{-1}$. Ushomirsky, Cutler et al. 2000

Is NS crust really elastic?

The STRESS tensor and the strain tensor $\epsilon_{\mu\nu}$ can be expressed in cartesian coord. (fixed V)

$$\sigma_{\alpha\beta} = C_{\alpha\beta xx}\epsilon_{xx} + 2C_{\alpha\beta xy}\epsilon_{xy} + 2C_{\alpha\beta xz}\epsilon_{xz} + C_{\alpha\beta yy}\epsilon_{yy} + 2C_{\alpha\beta yz}\epsilon_{yz} + C_{\alpha\beta zz}\epsilon_{zz}$$

as $\epsilon_{\mu\nu} \to 0$ the stress vanishes according to Hooke's law.

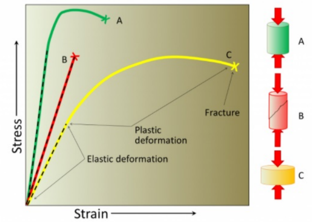

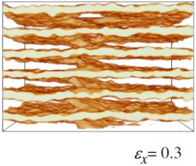

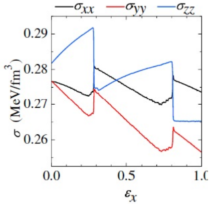

Caplan et al., 2018.

Oscillation modes

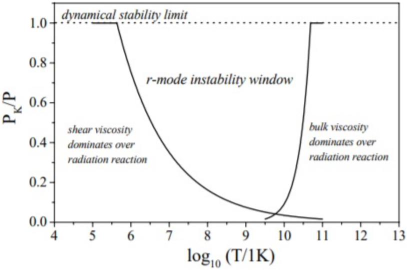

Fig. 3. The critical rotation rates at which shear viscosity (at low temperatures) and bulk viscosity (at high temperatures) balance gravitational radiation reaction due to the r-mode current multipole. This leads to the notion of a "window" in which the r-mode instability is active. The data in the figure is for the $l = m = 2$ r-mode of a canonical neutron star ($R = 10$ km and $M = 1.4M_\odot$ and Kepler period $P_K \approx 0.8$ ms).

Andersson and Kokkotas, 2010.

Additional coefficients in NS crust-core: shear viscosity

Kubo formulas for time correlations allow obtaining shear viscosity

$$\eta = \frac{\beta}{V} \int_0^{\infty} \langle \sigma_{xy}(t) \sigma_{xy}(0) \rangle \, dt$$

The dissipation timescale of r-modes due to the presence of the Ekman layer roughly follows from

$$t_{\mathrm{Ek}} \approx \frac{t_{\mathrm{sv}}}{\sqrt{Re}}$$

where $Re = \rho_b R_b^2 \Omega / \eta$ is the Reynolds number (the ratio between the Coriolis force and viscosity)
R_b and ρ_b are the location of, and density in the Ekman layer (base of the NS crust).

Additional coefficients in NS crust: bulk viscosity

bulk viscosity

$$\xi = \frac{\beta}{9V} \sum_{\alpha,\beta} \int_0^\infty \langle \sigma_{\alpha\alpha}(t) \sigma_{\beta\beta}(0) \rangle \, dt$$

$$\left. \frac{dE}{dt} \right|_{\mathrm{bv}} = - \int \zeta |\delta\sigma|^2$$

where $\delta\sigma$ is the expansion associated with the mode, defined by

$$\delta\sigma = -i\omega_r \frac{\Delta\rho}{\rho} = -i\omega_r \frac{\Delta p}{\Gamma p}$$

Kilonovae and GW: multimessenger signal in BNS will probe NS crust

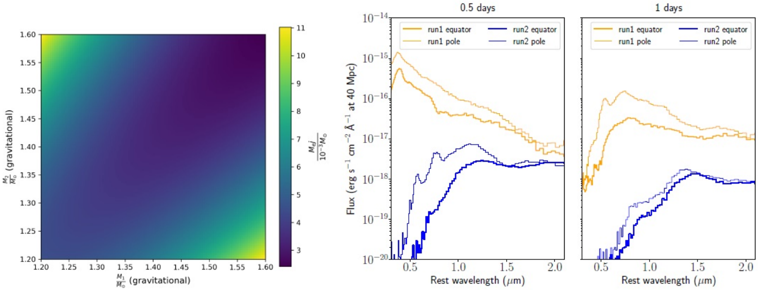

Figure 2 – (left) Ejected mass from simulation data [10]. (right) Simulated flux for a BNS merger using DD2 (run 1) and SFHo (run 2) EoS at 40 Mpc for polar and equatorial view angles at 0.5 d (left) and 1 d (right) after the merge.

MAAT @ GTC Prada et al., https://arxiv.org/abs/2007.01603

Conclusions

- NSs crust is an interesting place to develop axial asymmetries capable of powering GW emission.
- Microscopic simulations of neutron rich matter can provide a richer description of stresses in the crust due due to dynamical instabilities in an isolated object or binary
- Outer crust based on OCP description is a meaningful approximation to a multiple component hadron system.
- Preliminary analysis indicate in-medium effects must not be discarded and non-linear deformations may follow.

THANK YOU